JOURNAL OF GEOPHYSICAL RESEARCH, VOL. 115, D00I12, doi:10.1029/2009JD012359, 2010

First evidence of a 27 day solar signature in noctilucent cloud occurrence frequency

C. E. Robert,[1] C. von Savigny,[1] N. Rahpoe,[1] H. Bovensmann,[1] J. P. Burrows,[1] M. T. DeLand,[2] and M. J. Schwartz[3]

Received 30 April 2009; revised 24 September 2009; accepted 28 September 2009; published 30 March 2010.

[1] This paper presents evidence of a connection between the 27 day modulation of the solar activity and noctilucent cloud (NLC) occurrence frequency as measured by the Scanning Imaging Absorption Spectrometer for Atmospheric Chartography (SCIAMACHY) and solar backscatter ultraviolet (SBUV) instruments. Observations show anticorrelations significant at the 90% confidence level between noctilucent cloud occurrence rate anomalies and Lyman-α irradiance variation during several seasons in both hemispheres. A superposed epoch analysis confirms these results and also reveals a clear recurrence pattern in noctilucent clouds occurrence anomalies with a $\sim$27 day period. The superposed epoch analysis also shows that the maximum NLC response in the Northern Hemisphere is clearly localized at 0 day phase lag, while in the Southern Hemisphere the maximum response is broader and occurs at 0 $\pm$ 2 day phase lag. Microwave Limb Sounder mesospheric products suggest that the more likely driver for the variation in NLC occurrence is temperature instead of water vapor, but the mechanisms responsible for the observed variations are not yet fully understood.

Citation: Robert, C. E., C. von Savigny, N. Rahpoe, H. Bovensmann, J. P. Burrows, M. T. DeLand, and M. J. Schwartz (2010), First evidence of a 27 day solar signature in noctilucent cloud occurrence frequency, *J. Geophys. Res.*, *115*, D00I12, doi:10.1029/2009JD012359.

1. Introduction

[2] Noctilucent clouds (NLC), also known as polar mesospheric clouds (PMC), are atmospheric phenomena usually occurring poleward of 50° during the summer season. The extremely low temperatures ($\sim$130 K) and enhanced water vapor content ($\sim$3 ppm) near the summer mesopause lead to large saturation ratios ($\sim$100) and consequently to the formation of water ice aerosols [*Hervig et al.*, 2001]. It is still not clear what preexisting cores act as nuclei for the formation of NLC [*Rapp and Thomas*, 2006; *Gumbel and Megner*, 2009], if indeed heterogenous nucleation is required [*Zasetsky et al.*, 2009]. The NLC particles usually grow up to typical sizes of several tens of nanometers [*Gumbel et al.*, 2001; *Karlsson and Rapp*, 2006; *Robert et al.*, 2009] by direct deposition of water vapor on their surface. An ensemble of such particles forms a layer of roughly 1 km in vertical extent at altitudes of about 83 km [*Fiedler et al.*, 2003] and has an ice particle density on the order of 10^2 cm^{-3} at the cloud peak brightness [*Baumgarten et al.*, 2007]. NLC particles are transported by winds and settle under the action of gravity, and eventually sublimate when reaching subsaturated regions. A typical NLC season lasts from beginning of June until the end of August in the Northern Hemisphere and from beginning of December until the end of February in the Southern Hemisphere [*Thomas and Olivero*, 1989]. NLC are considered to be indicators of the state of the mesosphere [*Thomas and Olivero*, 2001], and observing their temporal and spatial variation can tell us more about phenomena taking place in this remote region of the Earth's atmosphere.

[3] NLC are affected by many different atmospheric processes such as gravity waves [e.g., *Gerrard et al.*, 2004; *Chandran et al.*, 2009], planetary waves [e.g., *Merkel et al.*, 2003; *von Savigny et al.*, 2007; *Merkel et al.*, 2008] and interhemispheric coupling [*Karlsson et al.*, 2007, 2009]. The SBUV instruments on board various NOAA satellites have been an invaluable source of information, providing NLC properties since 1979. As a result of this lengthy data record, it was possible to assess the impact of the 11 year solar cycle on NLC activity, showing significant anticorrelation between the occurrence frequency and the Lyman-α irradiance in both hemispheres [*DeLand et al.*, 2003], with a stronger anticorrelation in the Northern Hemisphere. *Hervig and Siskind* [2006] confirmed these findings using the HALOE instrument data set and showed the variation in NLC properties to be a consequence of temperature and water vapor changes in the upper mesosphere. Moreover, once the effect of the solar activity is removed from the SBUV time series, a positive secular trend of up to 20% was observed over the last 27 years in both NLC occurrence and albedo [*Shettle et al.*, 2009; *DeLand et al.*, 2007]. It has been argued that this

[1] Institute for Environmental Physics and Remote Sensing, University of Bremen, Bremen, Germany.
[2] Science Systems and Applications, Inc., Lanham, Maryland, USA.
[3] Jet Propulsion Laboratory, California Institute of Technology, Pasadena, California, USA.

0148-0227/10/2009JD012359$09.00

long-term change in NLC properties could be caused by an enhanced radiative cooling of the upper atmosphere due to a rise in greenhouse gas concentration as well as an increase in mesospheric water vapor concentrations [*Olivero and Thomas*, 2001; *Grygalashvyly and Sonnemann*, 2006], although most measurements do not support the hypothesis of a significant long-term temperature decrease near the mesopause [*Lübken*, 2000; *Beig et al.*, 2003].

[4] While the effect of the 11 year solar cycle on NLC is fairly well established, there is no peer-reviewed publication on the consequences of the quasi 27 day variation of the solar irradiance on NLC properties. This short-term UV flux variability, the result of the Sun's differential rotation, has a mean amplitude at 121.6 nm which corresponds to about 25% that of the 11 year solar cycle [*Woods et al.*, 2000], and varies considerably with solar activity itself so that it is larger during solar maximum and vice versa. Because the magnitude of this signal is not negligible compared to that of the 11 year solar cycle, it could conceivably affect the state of the upper mesosphere and consequently, the formation of NLC.

[5] The difficulty of the task lies in the detection of this signal during the short NLC season. If one conserves only the season's core containing approximately 90% of the total NLC detections, about 70 days are left to detect a 27 day signal. Moreover, as described before, many other processes with no direct link to the solar irradiance impact NLC, and so the search for a connection between NLC and solar activity will invariably be affected by these. The proxy for NLC activity must therefore be chosen with care so as to reflect best the effect that the solar radiation could have on NLC and maximize the population sampled. Among the many alternatives of possible NLC properties, the daily occurrence frequency, averaged zonally and over a latitude range of 60°–80° was chosen as a good indicator of NLC activity. It has the advantage of being simple, easily retrieved with few assumptions made and available from both SCIAMACHY and SBUV. The NLC albedo, used in many SBUV studies [*DeLand et al.*, 2007] could be employed as well, but because it is strongly correlated to the occurrence frequency for SBUV data, the conclusions drawn from a cross-correlation analysis based on either parameter should be similar. Moreover, SCIAMACHY albedo computation would require making assumptions on the particle size distribution of the NLC and would be quite sensitive to these assumptions because of the limb-viewing geometry. Other possible proxies of NLC activity would be the brightness peak altitude, the particle size and ice water content, which have the advantage of being real physical properties of NLC but usually require more assumptions to be made or cannot be measured accurately by either SCIAMACHY or SBUV.

[6] In this work, we investigate the effect of the 27 day solar flux variation on NLC occurrence frequency in both hemispheres using NLC data sets from the SCIAMACHY and SBUV instruments. Cross-correlation plots of solar Lyman-α irradiance and NLC occurrence frequency anomalies are presented for years 2002–2009 for SCIAMACHY and 1979–2006 for SBUV. Results obtained through a superposed epoch analysis of the solar forcing on NLC occurrence frequency are also shown in order to substantiate the relationship between these geophysical parameters. In connection with this analysis, we also examine MLS Aura mesospheric temperature and H_2O volume mixing ratios for the summer seasons 2005–2007.

2. Data Sets and Instrumentation

2.1. Lyman-α Composite Time Series

[7] In order to study the effect that solar variability has on NLC properties, we need a proxy of the solar activity. In this paper, we use the Lyman-α flux which is known to interact with the Earth's atmosphere chiefly at altitudes between 70 and 110 km, where it dissociates oxygen and water vapor and ionizes nitric oxide to form the ionosphere's D layer. It is also superior to the ground-based solar 10.7 cm radio flux measurements because, unlike the latter, it can still register the 27 day variation during quiet Sun conditions [*Barth et al.*, 1990]. Another reason for using the Lyman-α flux as a proxy is the availability of a time series which goes back to 1947. The data set was put together by *Woods et al.* [2000] by combining measurements from different satellites and using prediction from proxy models to fill the gaps between the different spaceborne missions. The uncertainty of the Lyman-α irradiance is estimated at 10% and is mainly due to the composite nature of the time series. The latest version of the data is available online from the Lasp Interactive Solar Irradiance Datacenter or LISIRD at http://lasp.colorado.edu/lisird and is updated weekly using TIMED SEE and SORCE SOLSTICE solar irradiance measurements.

2.2. SCIAMACHY on Envisat

[8] Scanning Imaging Absorption Spectrometer for Atmospheric Chartography (SCIAMACHY) is a research instrument on board the European satellite Envisat, launched in March 2002. It orbits the Earth Sun-synchronously with a descending equator crossing time of 1000 local time and a 83°S–83°N latitude coverage. SCIAMACHY observes the Earth's atmosphere in three different viewing geometries (limb, nadir and occultation) in the 230–2400 nm spectral range. In limb mode, SCIAMACHY scans the atmosphere vertically from 0 to 92 km in steps of 3.3 km and measures radiation coming from a field of view of 3 km vertical, ~400 km along track and 960 km across track.

[9] Since the nanometer-sized NLC particles scatter efficiently the Sun's incoming UV radiation, our detection algorithm looks for a peak or a strong gradient in limb radiance between 76 and 88 km altitude at different wavelengths. More information on NLC detection and retrieval from SCIAMACHY is provided by *Robert et al.* [2009]. The present NLC data set is based on fully calibrated SCIAMACHY level 1 data version 6.03.

2.3. SBUV on NOAA

[10] The Solar Backscatter Ultraviolet instrument (SBUV), a sensor designed to measure atmospheric ozone on a global scale, was introduced in 1978 on board the NIMBUS-7. The instrument measures the Earth radiance as well as the solar irradiance at 12 discrete wavelengths between 252 and 340 nm. An improved iteration of the instrument (SBUV/2) was later part of the NOAA-9, NOAA-11, NOAA-14, NOAA-16, NOAA-17 and NOAA-18 platforms so that, altogether, more than 30 years of operational data are available. Although primarily used

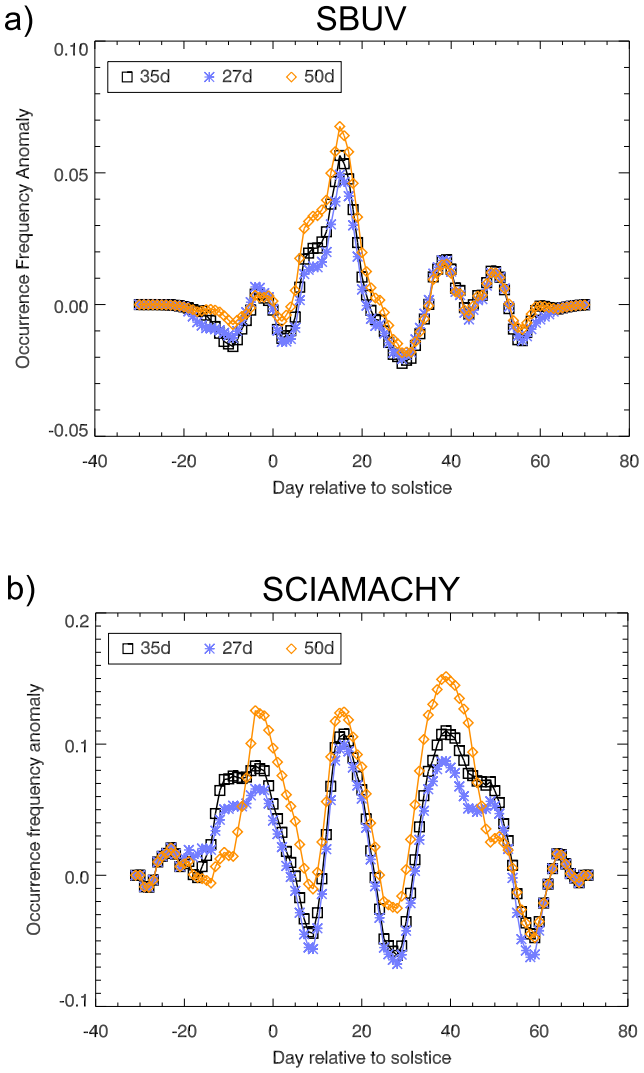

Figure 1. Anomalies calculated using the moving average method with a 27, 35, and 50 day boxcar for (a) SBUV and (b) SCIAMACHY zonally averaged data between 60° and 80° latitude. While the amplitude of the anomalies can change by a few percent, this will not affect the correlation analysis significantly since the spectral features remain the same across all curves.

to retrieve ozone profiles, *Thomas et al.* [1991] used the information available in the first five channels (252.0–292.3 nm) to detect NLC events and determine their albedo, i.e., the ratio of the measured NLC radiance and the solar radiance at a given wavelength. NLC can be identified in the SBUV data set due to their enhanced scattering of UV radiation, which has a different wavelength dependence than a decrease in ozone. The albedo measured with a NLC in the field of view will be larger than the average value, and this is basically how a NLC can be detected, although other conditions must be fulfilled in order to minimize the number of "false positive" detections. More information about the NLC detection algorithm used to produce the data set employed in this study is provided by *DeLand et al.* [2003].

2.4. MLS on Aura

[11] The Microwave Limb Sounder (MLS) measures the thermal microwave limb emissions from atmospheric species in five spectral regions from 115 GHz to 2.5 THz [*Waters et al.*, 2006]. It is on board the Aura spacecraft, launched 15 July 2004 in a Sun-synchronous orbit with a 13.45 LT ascending equator crossing time. MLS scans the atmosphere vertically from the ground to ~90 km, and its vertical scan rate varies with altitude, being faster in the upper regions of the atmosphere and resulting in poorer vertical resolution in the mesosphere.

[12] Measurements of temperature and H_2O, among other species, are done using digital autocorrelator spectrometers with a resolution of 0.15 MHz to measure narrow spectral lines at atmospheric pressures below 1 hPa, important for measurements in the middle atmosphere. The retrieval of the temperature profile is based on measurements of the thermal emission of O_2 near 118 and 234 GHz [*Schwartz et al.*, 2008], while the H_2O is retrieved from the emissions at 183.31 GHz [*Lambert et al.*, 2007].

[13] In this work, we use the MLS Level 2 geophysical product version 2.2. The spatial resolution for MLS H_2O product in the mesosphere is about 13 (vertical) × 400 (horizontal along track) × 7 km (horizontal cross track), with a 180% precision and a minimum measurable H_2O mixing ratio of 0.1 ppmv. Similarly, the resolution of a single temperature profile is about 15 × 220 × 6 km and has a 2.5 K precision in the mesosphere.

3. Data Analysis

3.1. Anomalies

[14] The NLC occurrence rates vary strongly during the 12 weeks of a typical NLC season and the removal of this seasonal variation is imperative for the appropriate computation of the anomalies which will be used for the correlation analysis. Different approaches exist to remove the seasonal component in a time series and it is important to make sure that the results obtained are not dependent on that particular preprocessing of the data set.

[15] One popular method to calculate anomalies is to transform the original signal in the frequency domain, multiply the spectra by an appropriate high-pass filter and transform that signal back in the time domain. Another possibility is to simply remove the entire season running mean of the signal (calculated using a given boxcar length) from the original signal. The length of the boxcar is chosen so as to get rid of the large seasonal modulation while the variations on shorter time scales are ideally not altered. A comparison of anomalies calculated using different boxcar lengths shows that the results are only slightly dependent on the procedure employed. Figure 1 shows examples of anomalies calculated using a 27, 35 and 50 day moving averages for SBUV and SCIAMACHY data. It is apparent that SCIAMACHY anomalies are more sensitive to the boxcar length than the SBUV data. This is a result of the larger sensitivity of SCIAMACHY to NLC, which in turn leads to a larger dynamical range of the NLC occurrence frequency and thereby an enhanced seasonal component which can be more difficult to remove. However, for both instruments, the amplitude of the anomalies only change by a few percent and the overall spectral characteristics are

almost identical regardless of the boxcar length used to calculate the anomalies. This should ensure that the conclusions drawn from a cross-correlation analysis using any of these curves as reference will be the same.

[16] We favor the running mean approach in this work because it handles missing data points without difficulty and is therefore straightforward to apply to all data sets. Anomalies are calculated using a 35 day boxcar as it was also employed in a similar study by *Hood* [1986] to analyze the response of ozone to short-term changes of solar UV flux. It should be noted that in order to smooth the anomalies, a final 5 day moving average is applied to them after the seasonal signal is removed, which can introduce a small shift of the signal in the time domain. Cross-correlation analysis of anomalies produced using different smoothing parameters show that this sometimes lead to an apparent phase lag of ±1 day.

3.2. Statistical Significance of Correlation

[17] Since this paper deals with the investigation of a connection between NLC occurrence and solar activity as well as other physical variables such as temperature and water vapor, cross correlation between different time series is a tool which will be used extensively. The statistical significance of the correlation cannot, in this case, be computed using Student's t distribution because adjacent observations of the time series are usually not independent from each other. Different techniques exist to evaluate the significance of the correlation between data sets [e.g., *Burnaby*, 1953; *Zwiers*, 1990], but few are able to deal appropriately with serial correlation.

[18] *Ebisuzaki* [1997] developed a simple method for the accurate computation of the correlation coefficient's statistical significance when dealing with autocorrelated time series. The procedure is similar to bootstrapping [*Bühlmann*, 2002] in that it takes the original data set and produces a sample of the population time series with the same mean and variance by random resampling. This sample can then be used to produce a statistical distribution of the correlation coefficient, providing an estimate of the likelihood of obtaining the correlation coefficient calculated for the original time series. However, mere permutation of the data set in the time domain does not account for its original serial correlation. Ebisuzaki realized that and converted the original data set in the frequency domain, produced a sample of the population by adding a random phase to each frequency component and converting back in the time domain. The data set obtained in this fashion has the same autocorrelation as the original one, which is what is needed for an unbiased statistical test for time series.

[19] In this paper, the confidence level of the statistical test for the correlation coefficient was set to 90%. While this figure may seem low in comparison with similar research, we justify its use by the fact that we do not expect all NLC occurrence anomalies to be explained by the Lyman-α variation alone. Many different mechanisms can be responsible for variation of the NLC occurrence throughout the season, but we are still looking for a correlation of some kind, and 90% confidence level seems fair in this context.

3.3. Superposed Epoch Method

[20] The response of the NLC occurrence to the 27 day cycle is not expected to be larger than other competing processes so we are in the situation where the response signal is potentially buried in random noise. The superposed epoch analysis, also sometimes referred to as compositing or Chree analysis, is a method used to investigate the response of a geophysical parameter in relation to some forcing, and is particularly well suited for this kind of situation. Since its introduction by *Chree* [1912, 1913], this type of analysis has been used extensively and in many different disciplines [*Severny et al.*, 1976; *Scherrer et al.*, 1979; *Mass and Portman*, 1989; *Lühr et al.*, 1998], especially in connection with solar periodicities.

[21] The procedure consists in defining so-called epochs in the response time series based on key events taking place in the forcing time series. In this study, we want to see whether the 27 day solar irradiance variation has an effect on the NLC occurrence frequency. We therefore catalogue all key events in the Lyman-α anomaly time series (in our case whenever we have a clear maximum or minimum in the amplitude of the 27 day cycle) and look at the corresponding response in NLC occurrence frequency using a window of data points centered on each key date. We will use a window containing 61 days so that we can observe the NLC response 30 days before and 30 days after the key event. A matrix is constructed using this information by entering the NLC response as a function of time relative to the key date in each row (the central row corresponds to the key date, i.e., day 0). For every key event defined, a new row is added. In order to remove from the NLC occurrence anomalies the random noise contributed by other processes such as wave activity or possible interhemispheric coupling, we simply average all of these events column-wise, i.e., for each day relative to the key date. Given a large enough sample of key events, the causal response of the NLC occurrence frequency to the solar forcing, if indeed present, should emerge in the average while noise in the data should cancel out. The window will allow us to see what is the mean phase lag of the response relative to the forcing. To test if the calculated average response is statistically significant, a bootstrapping approach is used where we randomly define a large number of key dates samples and generate a probability distribution of the average responses of the NLC occurrence frequency anomalies calculated in this way.

4. SCIAMACHY Time Series

[22] The NLC occurrence rate anomalies measured by SCIAMACHY between 2002–2009 for both hemispheres are presented in Figure 2 along with the Lyman-α anomalies (dashed line). Cross-correlation plots of both time series are also shown for each year, with the horizontal dashed lines in the cross-correlation plot designating the correlation coefficient statistically significant at the 90% confidence level (both positive and negative correlation).

[23] For most years in the Northern Hemisphere (NH), we observe a strong anticorrelation between Lyman-α and SCIAMACHY NLC anomalies, particularly marked in 2004 and 2005. We find a statistically significant anticorrelation for years 2004, 2005 and 2007 (for 0 day lag), which indicates that there is less than 10% probability that this is simply due to chance. The results for the Southern Hemisphere (SH) show that seasons 2002–2003, 2004–2005, and 2008–2009 have a statistically significant anti-

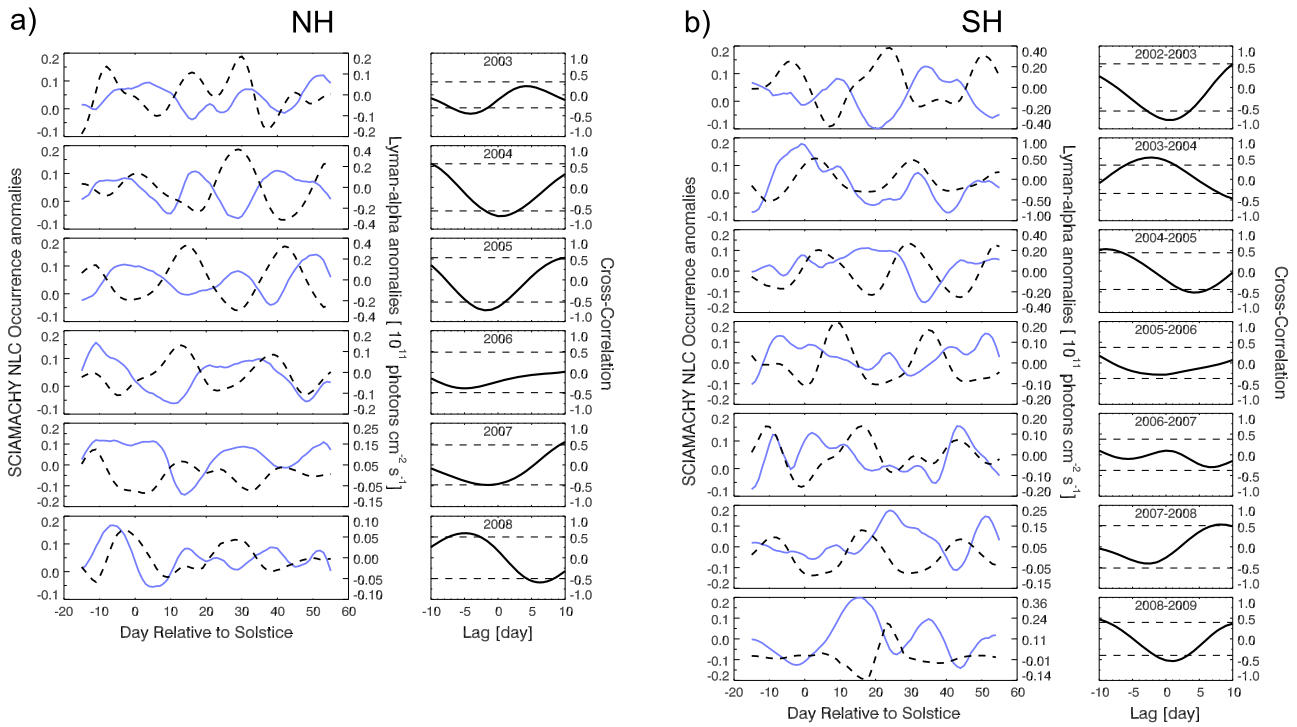

Figure 2. Time series of SCIAMACHY NLC occurrence anomalies (solid line) zonally averaged between 60° and 80° latitude and Lyman-α irradiance anomalies (dashed line) for different years and the associated cross-correlation function for (a) the Northern Hemisphere and (b) the Southern Hemisphere. Note that the vertical scale changes from year to year. The dashed lines in the cross-correlation plots represent the positive and negative correlation coefficient significant at the 90% confidence level calculated using the method explained in section 3.2.

correlation between solar activity and NLC occurrence, although we also see seasons displaying a positive correlation between Lyman-α and NLC anomalies (2003–2004 and 2006–2007).

[24] The minimum correlation coefficients are found to be at different phase lag depending on the season, sometimes happening after the peak in solar activity (positive lag) and sometimes occurring even before (negative lag). While a negative lag seems to contradict a causal relationship between the NLC anomalies and solar activity, we can imagine that other processes might take place which could alter the cross-correlation analysis and especially the location of the phase lag minimum. Overall, the cross-correlation minimum is in the vicinity of 0 day which suggests that short-term solar activity affects NLC on a very short time scale.

[25] The amplitude of the anomalies relative to the mean NLC occurrence frequency during the core of the season is 5–10% in the NH and 15–25% in the SH. We observe for both hemispheres that while the NLC occurrence rate anomalies are found to vary mostly between −0.1 and 0.1, the amplitude of the Lyman-α anomaly changes from year to year. It seems therefore that either the sensitivity of NLC occurrence rates to solar activity also changes from year to year or that the concept of sensitivity does not apply directly to the less physical NLC property that is the occurrence rate. Nevertheless, we expect the effect of solar activity on NLC occurrence to appear more conspicuously for seasons when the variation of the Lyman-α anomaly is large. Figure 3 shows the minimum correlation coefficient (within a ±1 day phase lag) against the standard deviation of the Lyman-α anomalies throughout the season for both hemispheres. The NH data show that for years with large

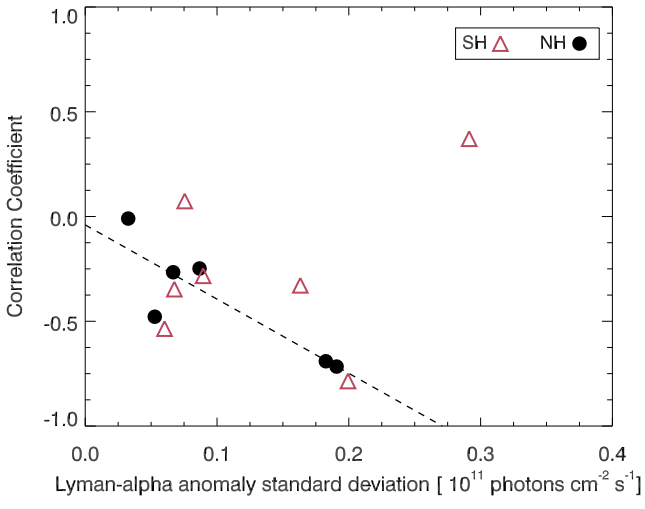

Figure 3. Minimum of the cross-correlation function of SCIAMACHY NLC occurrence with Lyman-α anomalies (in the phase lag interval [−1, 1]) for both hemispheres as a function of the Lyman-α anomaly standard deviation during the season. The dashed line represents a least-square fit through the NH data.

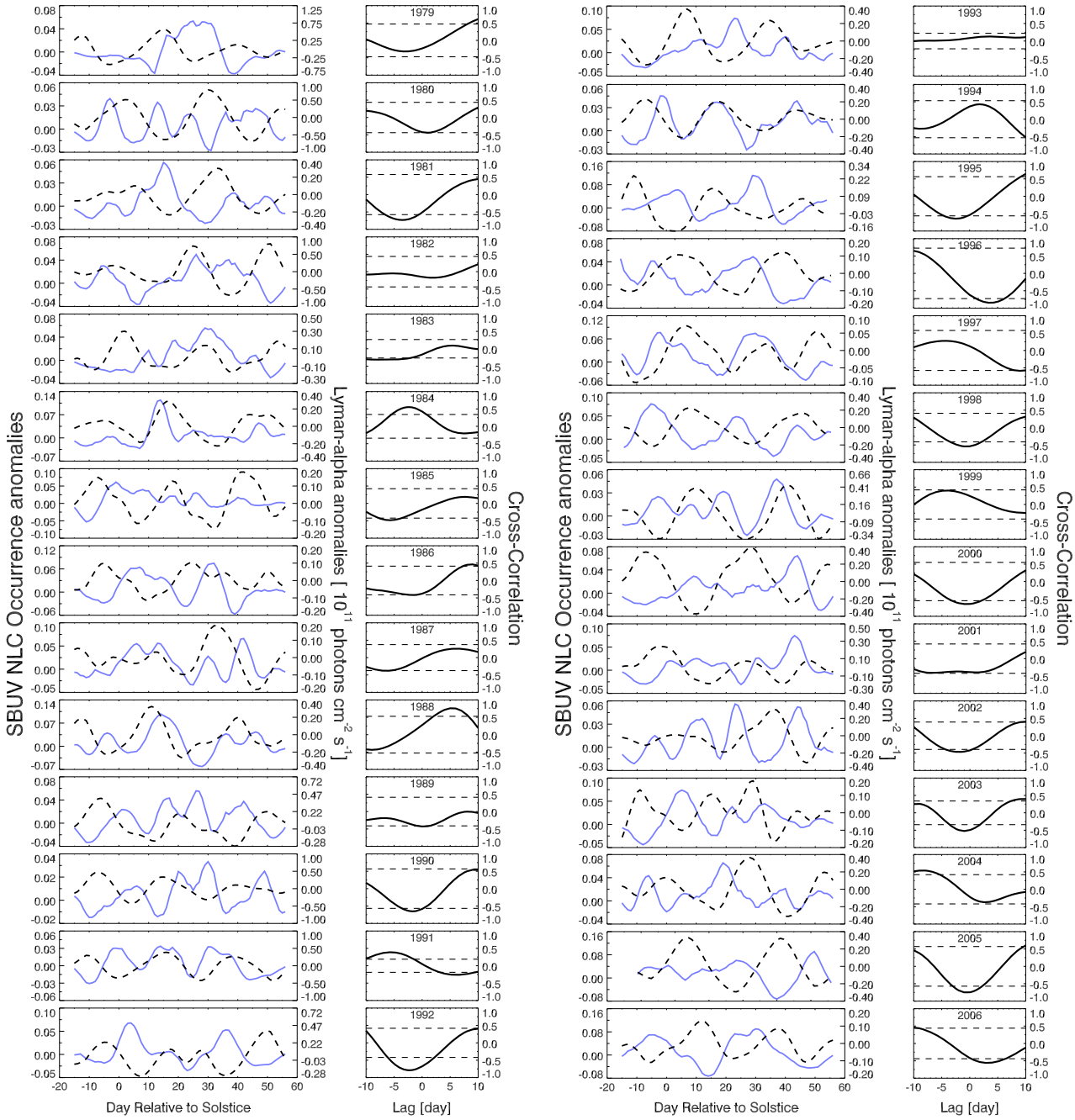

Figure 4. Time series plots of Northern Hemispheric SBUV NLC occurrence anomalies (solid line) zonally averaged between 60° and 80°N latitude and Lyman-α irradiance anomalies (dashed line) for different years and the associated cross-correlation function.

seasonal variations of the Lyman-α anomaly, a stronger anticorrelation is found between both time series. This effect is depicted more clearly by the dashed line, which is simply a linear fit through the NH data. A similar analysis for the SH data set does show a similar albeit weaker relationship, except for season 2003–2004 during which the Lyman-α irradiance varied strongly.

5. SBUV Time Series

[26] In order to substantiate the connection between NLC occurrence and solar activity established with the SCIAMACHY time series, we apply the same analysis as in section 4 to 28 years of SBUV data. As both time series overlap, it is also possible to see if the SCIAMACHY measurements are reproduced in the SBUV analysis. This will give a sound basis for rejecting the possibility that the correlation is due to an instrumental artifact.

[27] Figure 4 presents the NLC occurrence frequency anomalies (solid line) alongside the Lyman-α anomalies (dashed line) and a cross-correlation plot of both time series, for years 1979–2006 in the NH. Bear in mind the year to year variability of the vertical axis range of the anomalies, which maximizes the visible amplitude of both time series.

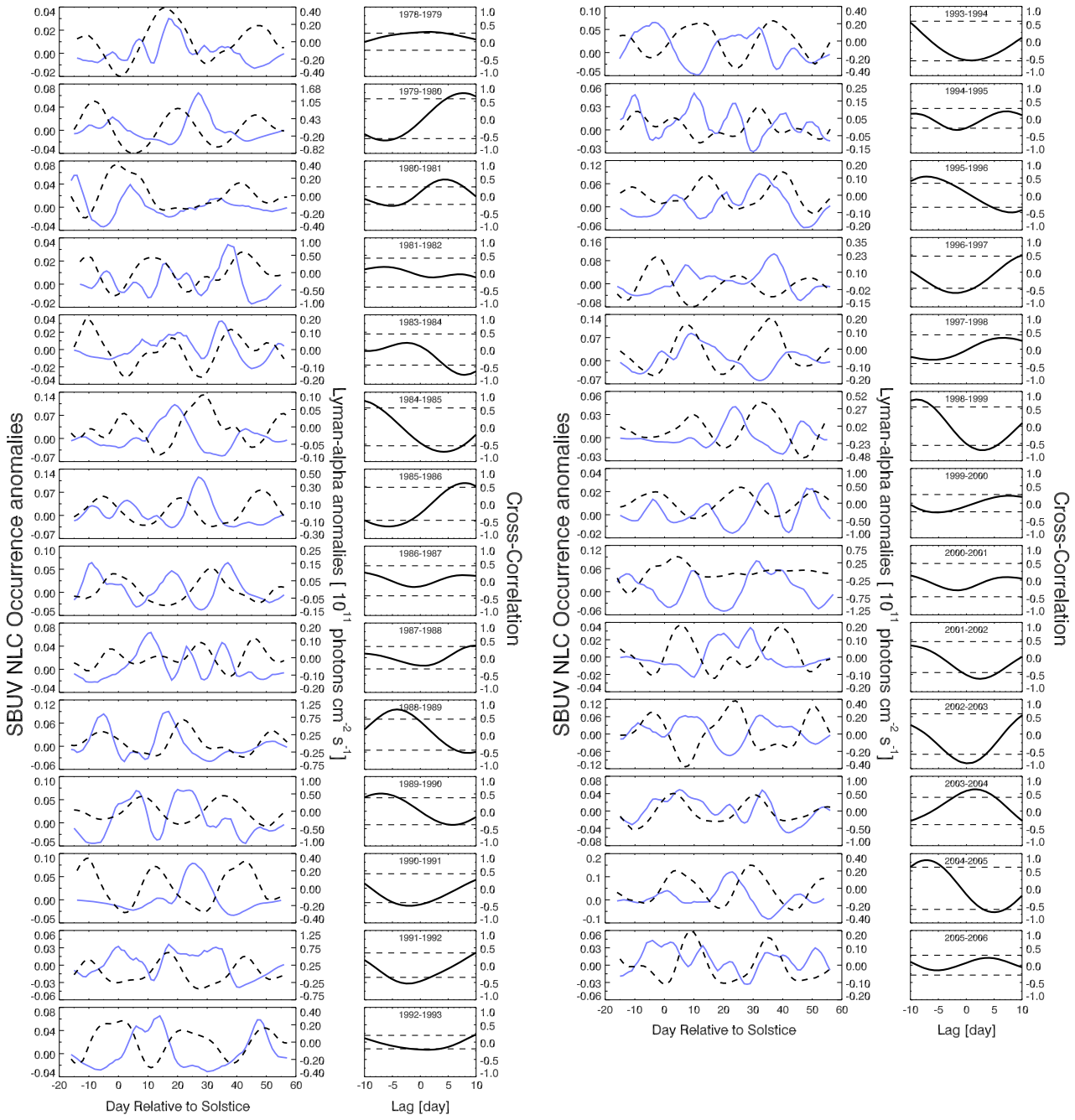

Figure 5. Time series plots of Southern Hemispheric SBUV NLC occurrence anomalies (solid line) zonally averaged between 60° and 80°S latitude and Lyman-α irradiance anomalies (dashed line) for different years and the associated cross-correlation function. Note that season 1982–1983 is missing.

Similarly to the SCIAMACHY results, many years show statistically significant anticorrelation, and the phase lag of the minimum correlation can be positive or negative and averages out to −0.3 day for all statistically significant negative correlations. NH seasons 1980, 1986, 1990, 1992, 1995, 1996, 1998, 2000, 2003, 2005 and 2006 show particularly clear anticorrelation between NLC anomalies and solar activity. Note also that for years of overlapping measurements between SCIAMACHY and SBUV, though there are slight discrepancies between the amplitude of both instrument's anomalies, the correlation analysis leads to similar results with significant anticorrelation for years 2003 to 2005. There are also years with positive correlation between both anomalies, the most noticeable being 1984, 1988, 1994 and 1997. The standard deviation of the anomalies correspond to about 20% of the NLC occurrence rate in the NH.

[28] SBUV data for the SH are presented in the same fashion in Figure 5. Note that we did not have enough data points for season 1982–1983 to conduct an appropriate analysis, which explains its absence from Figure 5. We can see that many SBUV seasons do show negative correlations between NLC and solar activity. Among the clearest exam-

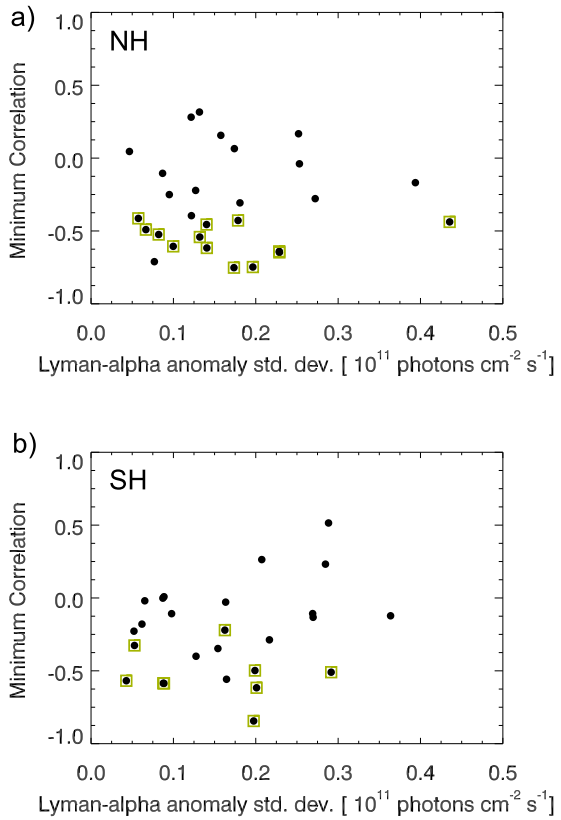

Figure 6. Minimum of the cross-correlation function of SBUV NLC occurrence with Lyman-α anomalies in the phase lag interval [−1, 1] as a function of the Lyman-α anomaly standard deviation during the season for the (a) NH and (b) SH. Data points outlined by square symbols represent anticorrelation statistically significant at the 90% confidence level.

ples of such anticorrelation are seasons 1984–1985, 1991–1992, 1993–1994, 1994–1995, 1996–1997, 1998–1999, 2001–2002 and 2002–2003. Only seasons 1983–1984, 1988–1989 and 2003–2004 show distinct positive correlation between the time series. The amplitude of the SH anomalies relative to the mean NLC occurrence frequency lies around 40% for all years.

[29] Figure 6 shows a scatterplot of the minimum correlation coefficient within a ±1 day phase lag interval as a function of the Lyman-α irradiance anomaly standard deviation for SBUV data in both hemispheres. Data points enclosed in a square symbol designate years for which the anticorrelation is statistically significant. One interesting feature of these plots is that the vast majority of data points have negative correlation coefficients, with mean correlation of −0.31 and −0.24 for the NH and SH, respectively. However, unlike the SCIAMACHY results of Figure 3, we cannot observe a clear linear relationship between the magnitude of the correlation and the amplitude of the Lyman-α anomalies seasonal variation.

6. Superposed Epoch Analysis

[30] Apart from the seasonally centric approach used previously in the cross-correlation analysis, we can also look at the data sets using the superposed epoch method described in section 3.3. This procedure takes advantage of long time series to improve the signal to noise ratio of the NLC occurrence frequency anomaly response to solar forcing.

[31] The analysis is carried out using two different types of event to determine the key dates in the time series: maximum and minimum of the Lyman-α anomalies. Only extrema with a clear localized peak were chosen in order to obtain unambiguous responses. We list 16 such events throughout the SCIAMACHY data set in the NH, and 18 in the SH. The mean response of the SCIAMACHY NLC occurrence frequency anomaly to solar forcing is shown in Figure 7 for both hemispheres. The solid line represents the response to conditions of maximum solar activity. We see that the NH NLC occurrence frequency is at a local minimum for 0 day phase lag, in good agreement with the anticorrelation of solar forcing and NLC occurrence frequency. This result is statistically significant at the 99.9% confidence level. It is also interesting to note that about 27 days after and before the key event takes place, a minimum in occurrence rate can also be observed which shows that there is indeed a recurrence of the signal after about 27 days, another confirmation of a solar signature in NLC occurrence frequencies. Not very surprisingly, the response of NLC to a minimum in solar

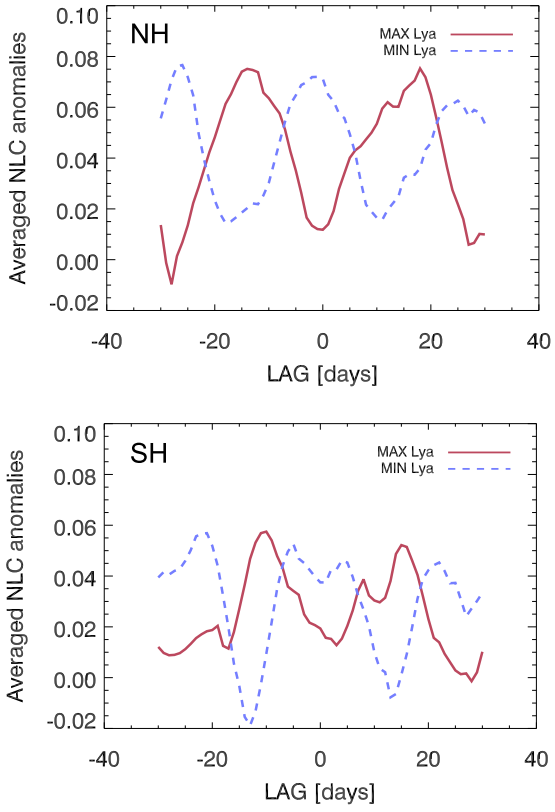

Figure 7. SCIAMACHY NLC occurrence frequency anomaly response to the solar forcing from the superposed epoch analysis for both hemispheres. The solid line shows the response to a maximum irradiance of the 27 day solar forcing while the dashed line corresponds to the NLC response to a minimum in solar irradiance. The NLC anomalies are calculated using zonally averaged occurrence frequency between 60° and 80° latitude.

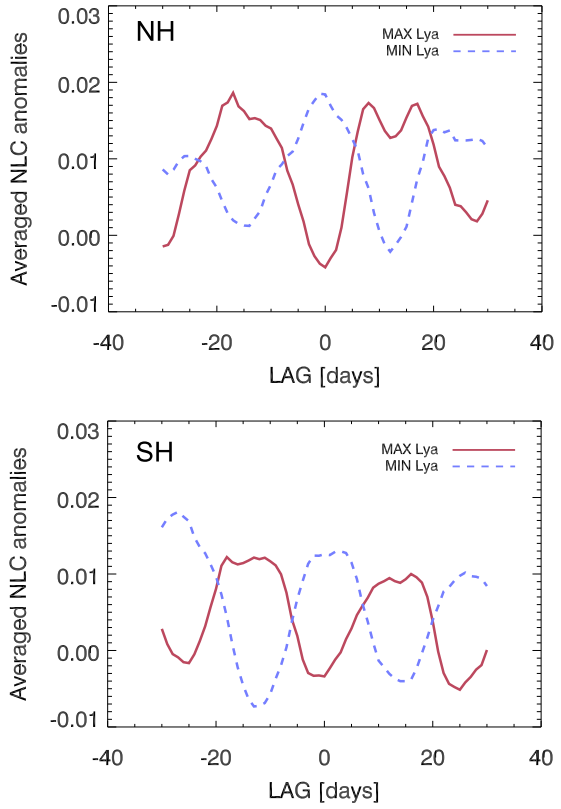

Figure 8. Superposed epoch analysis of the NLC occurrence frequency response to the 27 day solar forcing for SBUV data. The NLC anomalies are calculated using zonally averaged occurrence frequency between 60° and 80° latitude.

activity is consistent with this picture, with a phase lag of 0 day, a recurrence period between 25–30 days and a statistically significant anticorrelation at the 99.7% confidence level. Results in the SH, although showing some characteristics present in the NH curves such as recurrence, are noisier. For conditions of maximum solar irradiance, we obtain a local minimum in NLC occurrence frequency anomalies at a phase lag of +4 days. The situation is hazy around the occurrence of the solar minimum, with a local minimum at 0 day lag and local maxima at ±5 day lag. There is a strong negative response at phase lags of about ±13 days which is related to the maximum in the solar activity and is statistically significant at the 99% confidence level.

[32] The results of the analysis for the longer SBUV time series, containing 66 epochs in the NH and 62 in the SH, are presented in Figure 8. NLC response in the NH brings additional support that there is an anticorrelation between the 27 day solar forcing and NLC occurrence. The negative correlation is statistically significant at the 99.9% confidence level for the case of maximum solar activity and 99.3% for minima in the Lyman-α anomalies. The improved statistics of the SBUV data show that we also obtain similar results in the SH, although the phase lag of the peak response is not easily identified around the key event and spans a period of ±1 day in the case of solar maximum event, and ±3 days for solar minima. The anticorrelation is statistically significant at the 99.3% confidence level for maximum solar forcing and 98.8% for minimum.

7. Discussion

[33] The results from both SBUV and SCIAMACHY instruments show that there is strong evidence supporting the presence of a 27 day solar signature in NLC occurrence rates and that the signal is more clearly observed in the NH. NLC can be affected by changes in temperature and H_2O, and so the mechanisms responsible for the 27 day signature in NLC occurrence rates should impact either (or both) of these parameters.

7.1. Water Vapor

[34] Increased solar UV radiation should lead to enhanced photolysis of water vapor in the upper mesosphere [*von Zahn et al.*, 2004] and hence to a depletion of the H_2O molecules available for NLC formation, which could explain the observed anticorrelation of NLC occurrence with solar activity. To verify this possibility, we calculated the mesospheric water vapor anomalies from MLS absolute water vapor volume mixing ratio presented in Figure 9b. The contour plots of MLS H_2O mixing ratio anomalies (averaged over all longitudes and for latitudes 60°–80°) vertical profile are shown in Figure 10 for three entire NLC seasons and both hemispheres. Also shown in the plots are the Lyman-α anomalies throughout each season and the cross correlation of both H_2O (at 85 km) and Lyman-α.

[35] One of the main features of the contour plots is that the largest variability of H_2O in both hemispheres seems to be limited to altitudes above 80 km, with maximum amplitudes of 0.2–0.3 ppmv at NLC heights which corresponds to a variation of ~5% of the H_2O mixing ratio. The NH water vapor is positively correlated with the Lyman-α anomalies for year 2006 and 2007 with a phase lag of −1 and 0 day, respectively. The NH summer season 2005 shows little or no correlation between H_2O and Lyman-α for 0 day phase lag and a negative correlation for a 5 day lag. In the SH, H_2O is not correlated with the Lyman-α anomalies for a phase lag of 0 day.

[36] According to these results, the upper mesospheric water vapor is not anticorrelated with the Lyman-α anomalies and is even sometimes positively correlated for 0 day phase lag. Therefore, the water photolysis mechanism does not seem suitable to explain the 27 day modulation of NLC occurrence rate anomalies.

7.2. Temperature

[37] Solar variation could affect atmospheric temperatures by changing the photolysis of O_2 through the reaction $O_2 \rightarrow O + O$, increasing atomic oxygen concentrations and chemically producing more ozone $O_2 + O \rightarrow O_3$. The enhanced solar irradiance and ozone concentration will increase the radiative heating rates by ozone as well as chemical heating rates. Temperatures could also be indirectly influenced by the solar variation, for instance through dynamical effects. Similarly to water vapor, we calculated the anomalies from MLS absolute temperature measurements presented in Figure 9a.

[38] Figure 11 shows MLS temperature anomaly profiles during three NLC seasons in both hemispheres, along with the Lyman-α anomalies and the cross correlation of the

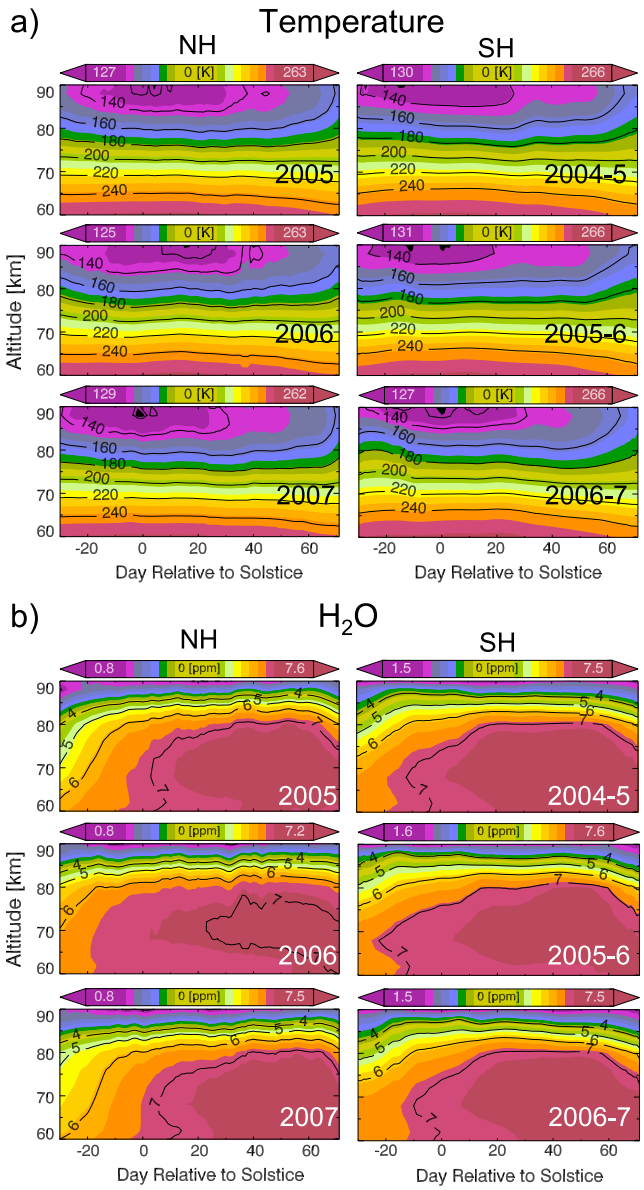

Figure 9. Vertical profile of MLS (a) temperature and (b) water vapor volume mixing ratio throughout NLC seasons 2005–2007 for both hemispheres, zonally averaged between 60° and 80° latitude.

solar activity proxy with temperature. For all NH seasons, we do see significant correlations between temperature and Lyman-α anomaly for a 0 day phase lag. The correlation is especially good for years 2005 and 2006, seasons for which our data shows significant anticorrelation between the solar signal and NLC occurrence rates anomaly. In the SH, the situation is not as clear. Temperature and Lyman-α do correlate positively (although not significantly) for seasons 2004–2005 and 2005–2006 but show no correlation for season 2006–2007. These results are in good agreement with the NLC and Lyman-α cross-correlation analysis and suggest that solar radiation modulates mesospheric temperatures, which in turn affect NLC occurrence rates.

[39] We observe also that while the amplitude of the temperature variation is about the same for all years, the 27 day solar UV forcing decreases from season to season. This is similar to what is observed in the NLC anomaly for both SCIAMACHY and SBUV. *Gruzdev et al.* [2009] state that this effect is also present in their model simulations of the effect of the 27 day solar UV forcing on middle-atmospheric temperatures, where the sensitivities of temperature to solar activity generally decrease when the forcing increases. Another interesting conclusion of this model study is that while there is a response in temperature to the 27 day solar cycle, it is intermittent and depends probably on the dynamical state of the atmosphere, something which can explain the absence of the signal in the NLC data set for some years.

[40] If temperature is indeed the dominant factor for the 27 day modulation, this could also explain the fact that the

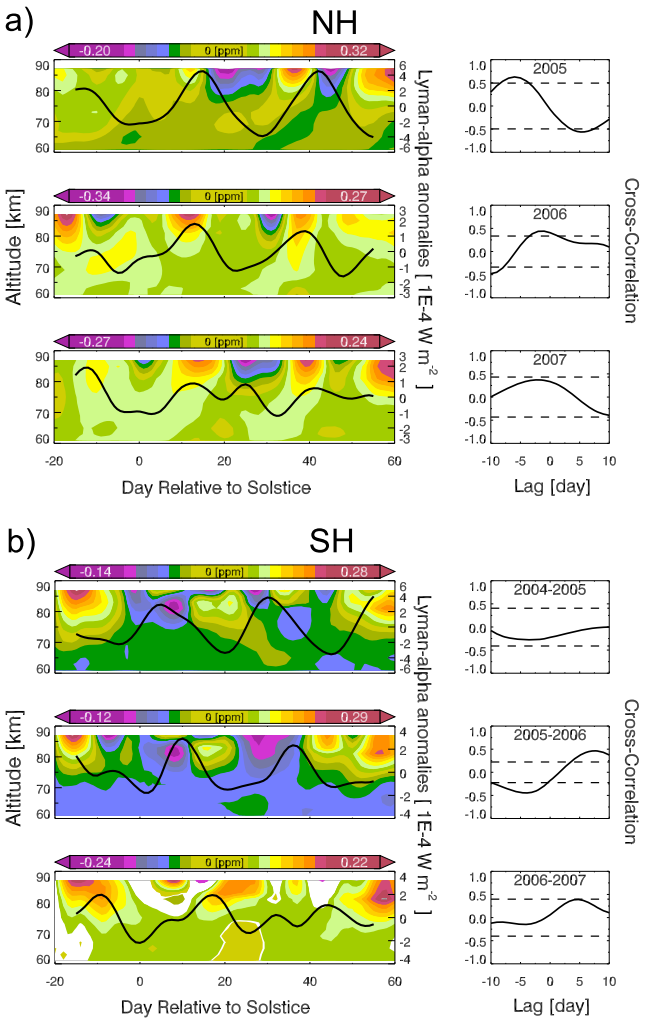

Figure 10. Vertical profile of MLS water vapor volume mixing ratio anomalies (zonally averaged between 60° and 80° latitude) throughout NLC seasons 2005–2007 (a) in the NH and (b) in the SH. Note that the color scale changes from year to year, as indicated by the legend above each contour plot. The solid line in the contour plots represent the Lyman-α anomalies throughout the seasons. The plots on the right-hand side show the cross-correlation function of the Lyman-α anomalies and H_2O anomalies at 85 km, and the dashed line represents the correlation and anticorrelation statistically significant at the 90% confidence level.

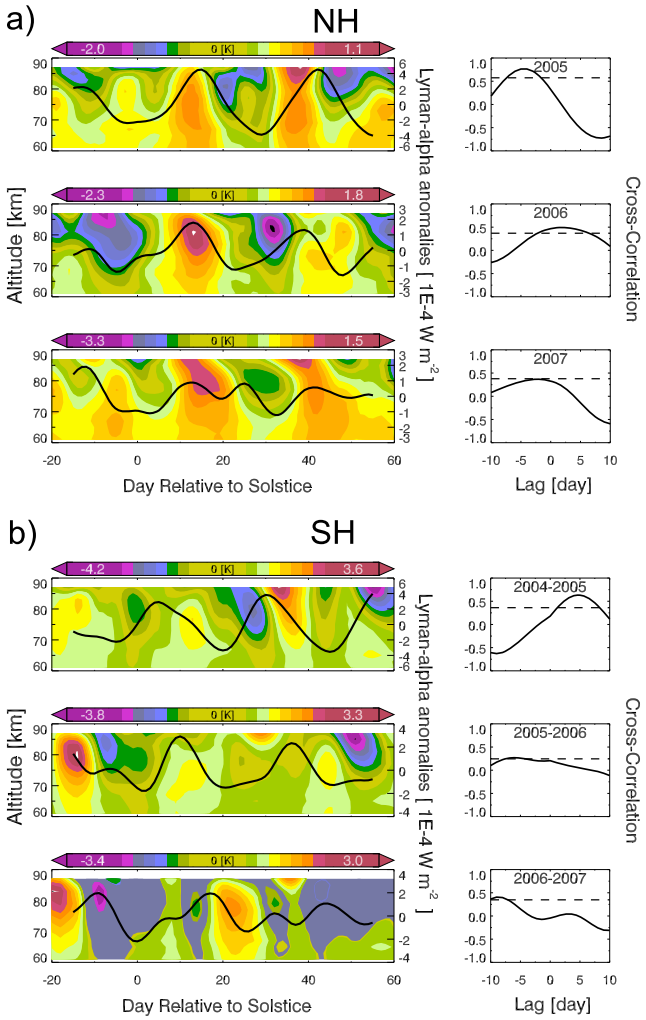

Figure 11. Contour plot of MLS temperature anomalies mean vertical profile (zonally averaged between 60° and 80° latitude) throughout the NLC seasons 2005–2007 along with the Lyman-α anomalies (a) in the NH and (b) in the SH, as in Figure 10.

signal is clearer in the NH than in the SH. Due to slightly higher temperatures (2–3 K) of the SH upper mesosphere [*Lübken and Berger*, 2007], the NLC population there exhibits a larger variability in frequency of occurrence than their NH counterpart [*Bailey et al.*, 2007]. NLC in the SH will also be more affected by the interhemispheric coupling [*Becker and Fritts*, 2006; *Karlsson et al.*, 2007] since stratospheric dynamics in NH is more unstable, and this may limit our ability to observe clearly the 27 day solar signature.

[41] Other than the results presented in this paper, a few references about a 27 day signal in mesospheric temperatures exist, albeit very few concerning the summer mesopause region at high latitudes. *Ebel et al.* [1986] report observations of temperature deviation of about 1.5 K at 80 km in the tropics, and argues that since the response to solar activity is mainly determined by the dynamical properties of the middle atmosphere, this means that the strongest perturbations should occur at middle and higher latitudes. Model results of the 27 day UV forcing of the atmosphere from *Zhu et al.* [2003] agree well with this argument, showing an increasing sensitivity of temperature to the solar UV forcing with increasing latitude and altitude. *Keating et al.* [1987] also measured a 27 day signal in temperature in the mesosphere, but with a maximum sensitivity at 70 km. Although specific results of all these studies do not always concur, they are nevertheless in agreement concerning the presence of a 27 day signal in middle-atmospheric temperatures which should affect the formation of NLC.

8. Conclusion

[42] In this paper, we presented NLC occurrence rate anomalies from SCIAMACHY showing a significant anticorrelation with solar Lyman-α anomalies for a 0 day phase lag in the NH. The SH seasons also showed anticorrelation as well as positive correlations for some seasons. The data record from SBUV-type instruments, which spans a much longer period than SCIAMACHY, also shows anticorrelation between Lyman-α anomalies and NLC occurrence rate anomalies (with phase lag $\approx$ 0) for a large number of years and for both hemispheres.

[43] The superposed epoch analysis was employed as a further tool to investigate the average response of NLC occurrence anomalies to the 27 day solar forcing. It strongly supported the hypothesis of a negative correlation between solar activity and NLC occurrence frequency, statistically significant at the 99% confidence level. The analysis also revealed a $\sim$27 day recurrence tendency in the NLC response which corroborates the presence of a 27 day signature in NLC occurrence frequency.

[44] The analysis of MLS mesospheric H_2O measurements during three NLC seasons shows that water vapor photolysis by short-term UV variation around 83 km cannot explain the NLC occurrence rate anomalies observed. The MLS temperature data on the other hand are positively correlated with the Lyman-α flux at NLC altitudes. This correlation is especially strong in the NH while the results of the SH are more variable, a feature also seen for NLC occurrences. Other studies also report a 27 day signature in middle-atmospheric temperatures either in observations or models, which supports our view that temperature is likely the main driver affecting the variation of NLC on the 27 day time scale. Future models of the 27 day signal in the summer mesosphere at high latitude should be able to reproduce these observations and hopefully describe the specific mechanisms responsible the 27 day signature in NLC.

[45] **Acknowledgments.** We would like to acknowledge the anonymous reviewers for their helpful comments and their suggestion of using the superposed epoch analysis. This work was supported by the German Ministry of Education and Research (BMBF), the German Aerospace Center (DLR), the DFG-CAWSES (project WAVE-NLC), and the University of Bremen (project ICAPS). SCIAMACHY is jointly funded by Germany, Netherlands, and Belgium. We are also indebted to ESA for providing SCIAMACHY Level 1 data.

References

Bailey, S. M., A. W. Merkel, G. E. Thomas, and D. W. Rusch (2007), Hemispheric differences in polar mesospheric cloud morphology observed by the SNOE, *J. Atmos. Sol. Terr. Phys.*, *69*, 1407–1418.

Barth, C. A., W. K. Tobiska, G. J. Rottman, and O. R. White (1990), Comparison of 10.7 cm radio flux with SME solar Lyman alpha flux, *Geophys. Res. Lett.*, *17*(5), 571–574.

Baumgarten, G., J. Fiedler, and G. von Cossart (2007), The size of noctilucent cloud particles above ALOMAR (69N, 16E): Optical modeling and method description, *Adv. Space Res.*, *40*, 772–784.

Becker, E., and D. Fritts (2006), Enhanced gravity-wave activity and interhemispheric coupling during the MacWAVE/MIDAS northern summer program 2002, *Ann. Geophys.*, *24*, 1175–1188.

Beig, G., et al. (2003), Review of mesospheric temperature trends, *Rev. Geophys.*, *41*(4), 1015, doi:10.1029/2002RG000121.

Bühlmann, P. (2002), Bootstraps for time series, *Stat. Sci.*, *17*(1), 52–72.

Burnaby, T. (1953), A suggested alternative to the correlation coefficient for testing the significance of agreement between pairs of time series, and its application to geological data, *Nature*, *172*, 210–212.

Chandran, A., D. Rusch, S. Palo, G. Thomas, and M. J. Taylor (2009), Gravity wave observations in the summertime polar mesosphere from the Cloud Imaging and Particle Size (CIPS) experiment on the AIM spacecraft, *J. Atmos. Sol. Terr. Phys.*, *71*, 392–400.

Chree, C. (1912), Some phenomena of sunspots and of terrestrial magnetism at Kew Observatory, *Philos. Trans. R. Soc., Ser. A*, *212*, 75–116.

Chree, C. (1913), Some phenomena of sunspots and of terrestrial magnetism part II, *Philos. Trans. R. Soc., Ser. A*, *213*, 245–277.

DeLand, M. T., E. P. Shettle, G. E. Thomas, and J. J. Olivero (2003), Solar backscattered ultraviolet (SBUV) observations of polar mesospheric clouds (PMCs) over two solar cycles, *J. Geophys. Res.*, *108*(D8), 8445, doi:10.1029/2002JD002398.

DeLand, M. T., E. P. Shettle, G. E. Thomas, and J. J. Olivero (2007), Latitude-dependent long-term variations in polar mesospheric clouds from SBUV version 3 PMC data, *J. Geophys. Res.*, *112*, D10315, doi:10.1029/2006JD007857.

Ebel, A., M. Dameris, H. Hass, A. H. Manson, and C. E. Meek (1986), Vertical change of the response to solar activity oscillations with periods around 13 and 27 days in the middle atmosphere, *Ann. Geophys.*, *4*, 271–280.

Ebisuzaki, W. (1997), A method to estimate the statistical significance of a correlation when the data are serially correlated, *J. Clim.*, *10*(9), 2147–2153.

Fiedler, J., G. Baumgarten, and G. von Cossart (2003), Noctilucent clouds above ALOMAR between 1997 and 2001: Occurrence and properties, *J. Geophys. Res.*, *108*(D8), 8453, doi:10.1029/2002JD002419.

Gerrard, A. J., T. J. Kane, J. P. Thayer, and S. D. Eckermann (2004), Concerning the upper stratospheric gravity wave and mesospheric cloud relationship over Sondrestrom, Greenland, *J. Atmos. Sol. Terr. Phys.*, *66*, 229–240.

Gruzdev, A. N., H. Schmidt, and G. P. Brasseur (2009), The effect of the solar rotational irradiance variation on the middle and upper atmosphere calculated by a three-dimensional chemistry-climate model, *Atmos. Chem. Phys.*, *9*(2), 595–614.

Grygalashvyly, M., and G. Sonnemann (2006), Trends of mesospheric water vapor due to the increase of methane—A model study particularly considering high latitudes, *Adv. Space Res.*, *38*, 2396–2401.

Gumbel, J., and L. Megner (2009), Charged meteoric smoke as ice nuclei in the mesosphere: Part 1—A review of basic concepts, *J. Atmos. Sol. Terr. Phys.*, *71*, 1225–1235.

Gumbel, J., J. Stegman, D. P. Murtagh, and G. Witt (2001), Scattering phase functions and particle sizes in noctilucent clouds, *Geophys. Res. Lett.*, *28*(8), 1415–1418.

Hervig, M., and D. Siskind (2006), Decadal and inter-hemispheric variability in polar mesospheric clouds, water vapor, and temperature, *J. Atmos. Sol. Terr. Phys.*, *68*, 30–41.

Hervig, M., R. E. Thompson, M. McHugh, L. L. Gordley, J. M. Russel III, and M. E. Summers (2001), First confirmation that water ice is the primary component of polar mesospheric clouds, *Geophys. Res. Lett.*, *28*(6), 971–974.

Hood, L. L. (1986), Coupled stratospheric ozone and temperature responses to short-term changes in solar ultraviolet flux—An analysis of Nimbus-7 SBUV and SAMS data, *J. Geophys. Res.*, *91*(D4), 5264–5276.

Karlsson, B., and M. Rapp (2006), Latitudinal dependence of noctilucent cloud growth, *Geophys. Res. Lett.*, *33*, L11812, doi:10.1029/2006GL025805.

Karlsson, B., H. Körnich, and J. Gumbel (2007), Evidence for interhemispheric stratosphere-mesosphere coupling derived from noctilucent cloud properties, *Geophys. Res. Lett.*, *34*, L16806, doi:10.1029/2007GL030282.

Karlsson, B., C. McLandress, and T. G. Shepherd (2009), Inter-hemispheric mesospheric coupling in a comprehensive middle atmosphere model, *J. Atmos. Sol. Terr. Phys.*, *71*, 518–530.

Keating, G., M. Pitts, G. Brasseur, and A. D. Rudder (1987), Response of middle atmosphere to short-term solar ultraviolet variations: 1. Observations, *J. Geophys. Res.*, *92*(D1), 889–902.

Lambert, A., et al. (2007), Validation of the Aura microwave limb sounder middle atmosphere water vapor and nitrous oxide measurements, *J. Geophys. Res.*, *112*, D24S36, doi:10.1029/2007JD008724.

Lübken, F. J. (2000), Nearly zero temperature trend in the polar summer mesosphere, *Geophys. Res. Lett.*, *27*(21), 3603–3606.

Lübken, F.-J., and U. Berger (2007), Interhemispheric comparison of mesospheric ice layers from the LIMA model, *J. Atmos. Sol. Terr. Phys.*, *69*, 2292–2308.

Lühr, H., M. Rother, T. Iyemori, T. L. Hansen, and R. P. Lepping (1998), Superposed epoch analysis applied to large-amplitude travelling convection vortices, *Ann. Geophys.*, *16*, 743–753.

Mass, C. F., and D. A. Portman (1989), Major volcanic eruptions and climate: A critical evaluation, *J. Clim.*, *2*(6), 566–593.

Merkel, A. W., G. E. Thomas, S. E. Palo, and S. M. Bailey (2003), Observations of the 5-day planetary wave in PMC measurements from the Student Nitric Oxide Explorer Satellite, *Geophys. Res. Lett.*, *30*(4), 1196, doi:10.1029/2002GL016524.

Merkel, A. W., R. R. Garcia, S. M. Bailey, and J. M. Russel III (2008), Observational studies of planetary waves in PMCs and mesospheric temperature measured by SNOE and SABER, *J. Geophys. Res.*, *113*, D14202, doi:10.1029/2007JD009396.

Olivero, J. J., and G. E. Thomas (2001), Evidence for changes in greenhouse gases in the mesosphere, *Adv. Space Res.*, *28*, 931–936.

Rapp, M., and G. E. Thomas (2006), Modeling the microphysics of mesospheric ice particles: Assessment of current capabilities and basic sensitivities, *J. Atmos. Sol. Terr. Phys.*, *68*, 715–744.

Robert, C. E., C. von Savigny, J. P. Burrows, and G. Baumgarten (2009), Climatology of noctilucent cloud radii and occurrence frequency using SCIAMACHY, *J. Atmos. Sol. Terr. Phys.*, *71*, 408–423.

Scherrer, P. H., J. M. Wilcox, V. A. Kotov, A. B. Severny, and T. T. Tsap (1979), Observations of solar oscillations with periods of 160 minutes, *Nature*, *277*, 635–637.

Schwartz, M. J., et al. (2008), Validation of the Aura Microwave Limb Sounder temperature and geopotential height measurements, *J. Geophys. Res.*, *113*, D15S11, doi:10.1029/2007JD008783.

Severny, A. B., V. A. Kotov, and T. T. Tsap (1976), Observations of solar pulsations, *Nature*, *259*, 87–89.

Shettle, E. P., M. T. Deland, G. E. Thomas, and J. J. Olivero (2009), Long term variations in the frequency of polar mesospheric clouds in the Northern Hemisphere from SBUV, *Geophys. Res. Lett.*, *36*, L02803, doi:10.1029/2008GL036048.

Thomas, G. E., and J. J. Olivero (1989), Climatology of polar mesospheric clouds: 2. Further analysis of Solar Mesosphere Explorer data, *J. Geophys. Res.*, *94*(D12), 14,673–14,681.

Thomas, G. E., and J. J. Olivero (2001), Noctilucent clouds as possible indicators of global change in the mesosphere, *Adv. Space Res.*, *28*, 937–946.

Thomas, G. E., R. D. McPeters, and E. J. Jensen (1991), Satellite observations of polar mesospheric clouds by the solar backscattered ultraviolet spectral radiometer: Evidence of a solar cycle dependence, *J. Geophys. Res.*, *96*(D1), 927–939.

von Savigny, C., C. E. Robert, H. Bovensmann, J. P. Burrows, and M. Schwartz (2007), Satellite observations of the quasi 5-day wave in noctilucent clouds and mesopause temperatures, *Geophys. Res. Lett.*, *34*, L24808, doi:10.1029/2007GL030987.

von Zahn, U., G. Baumgarten, U. Berger, J. Fiedler, and P. Hartogh (2004), Noctilucent clouds and the mesospheric water vapour: The past decade, *Atmos. Chem. Phys.*, *4*, 2449–2464.

Waters, J. W., et al. (2006), The Earth Observing System Microwave Limb Sounder (EOS MLS) on the Aura satellite, *IEEE Trans. Geosci. Remote Sens.*, *44*(5), 1075–1092.

Woods, T. N., W. K. Tobiska, G. J. Rottman, and J. R. Worden (2000), Improved solar Lyman alpha irradiance modeling from 1947 through 1999 based on UARS observations, *J. Geophys. Res.*, *105*(A12), 27,195–27,216.

Zasetsky, A. Y., S. V. Petelina, and I. M. Svishchev (2009), Thermodynamics of homogeneous nucleation of ice particles in the polar summer mesosphere, *Atmos. Chem. Phys.*, *9*, 965–971.

Zhu, X., J. Yee, and E. Talaat (2003), Effect of short-term solar ultraviolet flux variability in a coupled model of photochemistry and dynamics, *J. Atmos. Sci.*, *60*(3), 491–509.

Zwiers, F. W. (1990), The effect of serial correlation on statistical inferences made with resampling procedures, *J. Clim.*, *3*(12), 1452–1461.

H. Bovensmann, J. P. Burrows, N. Rahpoe, C. E. Robert, and C. von Savigny, Institute for Environmental Physics and Remote Sensing, University of Bremen, Otto-Hahn-Allee 1, D-28359 Bremen, Germany. (crobert@iup.physik.uni-bremen.de)

M. T. DeLand, Science Systems and Applications, Inc., 10210 Greenbelt Rd., Suite 400, Lanham, MD 20706, USA.

M. J. Schwartz, Jet Propulsion Laboratory, California Institute of Technology, 4800 Oak Grove Dr., Pasadena, CA 91109, USA.